

Lawrence Berkeley National Laboratory

Recent Work

Title

AMIDE PROTON SPIN-LATTICE RELAXATION IN POLYPEPTIDES: A FIELD-DEPENDENCE STUDY OF THE PROTON AND NITROGEN DIPOLAR INTERACTIONS IN ALUMICHROME

Permalink

<https://escholarship.org/uc/item/4zh8f380>

Author

Llinas, M.

Publication Date

1978-05-01

C.2

AMIDE PROTON SPIN-LATTICE RELAXATION IN POLYPEPTIDES:
A FIELD-DEPENDENCE STUDY OF THE PROTON AND
NITROGEN DIPOLAR INTERACTIONS IN ALUMICHROME

M. Llinás, M. P. Klein, and K. Wüthrich

May 1978

RECEIVED
LAWRENCE
BERKELEY LABORATORY

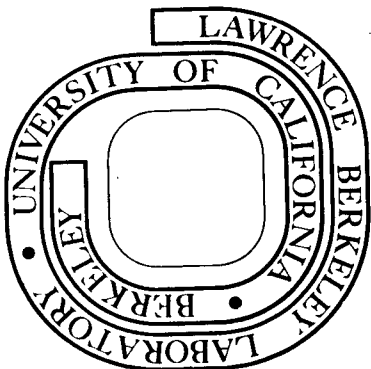
JUN 6 1978

LIBRARY AND
DOCUMENTS SECTION

Prepared for the U. S. Department of Energy
under Contract W-7405-ENG-48

TWO-WEEK LOAN COPY

*This is a Library Circulating Copy
which may be borrowed for two weeks.
For a personal retention copy, call
Tech. Info. División, Ext. 6782*



C.2

DISCLAIMER

This document was prepared as an account of work sponsored by the United States Government. While this document is believed to contain correct information, neither the United States Government nor any agency thereof, nor the Regents of the University of California, nor any of their employees, makes any warranty, express or implied, or assumes any legal responsibility for the accuracy, completeness, or usefulness of any information, apparatus, product, or process disclosed, or represents that its use would not infringe privately owned rights. Reference herein to any specific commercial product, process, or service by its trade name, trademark, manufacturer, or otherwise, does not necessarily constitute or imply its endorsement, recommendation, or favoring by the United States Government or any agency thereof, or the Regents of the University of California. The views and opinions of authors expressed herein do not necessarily state or reflect those of the United States Government or any agency thereof or the Regents of the University of California.

AMIDE PROTON SPIN-LATTICE RELAXATION IN POLYPEPTIDES: A FIELD-
DEPENDENCE STUDY OF THE PROTON AND NITROGEN DIPOLAR INTERACTIONS
IN ALUMICHROME.

M. Llinás,^{*} M. P. Klein, and K. Wüthrich

Chemical Biodynamics Laboratory, University of California,

Berkeley, California 94720 (M.Ll. & M.P.K.) and the

Institute of Molecular Biology and Biophysics, ETH-Hönggerberg,

8093 Zürich, Switzerland (M. Ll. & K. W.)

* Author to whom correspondence should be directed. Present Address:

Department of Chemistry, Carnegie-Mellon University, Pittsburgh, PA 15213.

ABSTRACT

The proton nmr spin-lattice relaxation of all six amides of deferriferrichrome and of various alumichromes dissolved in d_6 -dimethylsulfoxide, have been investigated at 100, 220 and 360 MHz. It is found that, depending on the type of residue (glycyl or ornithyl), the amide proton relaxation rates are rather uniform in the metal-free cyclohexapeptide. In contrast, the T_1 's are distinct in the Al^{3+} -coordination derivative. Similar patterns are observed in a number of isomorphous alumichrome homologues which differ in single site residue substitutions, indicating that the spin-lattice relaxation rate is mainly determined by dipole-dipole interactions within a rigid molecular framework rather than by the specific primary structures. Analysis of the data in terms of 1H - 1H distances (r) calculated from X-ray coordinates yields a satisfactory linear fit between T_1^{-1} and Σr^{-6} at the three magnetic fields. Considering the very sensitive r -dependence of T_1 , the agreement gives confidence, at a quantitative level, both on the fitness of the crystallographic model to represent the alumichromes' solution conformation and on the validity of assuming isotropic rotational motion for the globular metallopeptides. An extra contribution to the amide proton T_1^{-1} is proposed to mainly originate from the 1H - ^{14}N dipolar interaction: this was supported by comparison with measurements on an ^{15}N -enriched peptide. The nitrogen dipolar contribution to the peptide proton relaxation is discussed in the context of $\{^1H\}$ - 1H nuclear Overhauser enhancement (nOe) studies as, especially at high fields, it can be dominant in determining

the amide proton relaxation rates and hence result in a decreased effectiveness for the ^1H - ^1H dipolar mechanism to cause nOe's. From the slope and intersect values of T_1^{-1} vs. Σr^{-6} linear plots, a number of independent estimates of τ_r , the rotational correlation time, were derived. These and the field-dependence of the T_1 's yield a best estimate $\langle \tau_r \rangle \approx 0.37$ ns, in good agreement with $0.38 \text{ ns} \lesssim \langle \tau_r \rangle \lesssim 0.41 \text{ ns}$, previously determined from ^{13}C and ^{15}N spin-lattice relaxation data.

INTRODUCTION

In spite of the sensitivity advantage afforded by proton nuclear magnetic resonance (nmr) spectroscopy, studies of the ^1H spin-lattice relaxation time (T_1) have not enjoyed the popularity of, say, ^{13}C -nmr when investigating the conformational dynamics of polypeptides in liquid solution. This neglect derives for various reasons.

For the case of polypeptides and proteins dissolved in deuterated solvents, it is well substantiated that the proton spin-lattice relaxation processes are mostly mediated by intramolecular ^1H - ^1H interactions (1-3). In particular, for the case of isotropic molecular tumbling, the $^1\text{H}_i$ dipolar contribution to the $^1\text{H}_j$ relaxation rate (T_{1j}^{-1}) is governed by eq. (1)

$$\frac{1}{T_{1j}} = \frac{3}{2} \gamma_H^4 \hbar^2 I(I+1) \frac{4}{15} \frac{1}{r_{ij}^6} \left[\frac{\tau_r}{(1 + \omega^2 \tau_r^2)} + \frac{4\tau_r}{(1 + 4\omega^2 \tau_r^2)} \right] \quad (1)$$

where γ_H is the proton magnetogyric ratio, $I = 1/2$ is the proton spin, r_{ij} is the internuclear distance separating atoms H_i and H_j , τ_r is the overall molecular rotational correlation time, and $\omega = \gamma_H B$ is the angular precession frequency of the proton in the external polarizing magnetic field \vec{B} (4). Equation (1) can be rewritten

$$\frac{1}{T_{1j}} = A f(\omega, \tau_r) r_{ij}^{-6} \quad (2)$$

where $f(\omega, \tau_r)$ is the expression within brackets in eq. (1) and A contains the multiplicative constants. Equation (2) emphasizes the fact that at a predetermined \bar{B} ($\omega = \text{const.}$), for a given spherical molecule under defined temperature and solvent conditions ($\tau_r = \text{const.}$), the only variable left controlling the dipolar proton relaxation rate is the ${}^1\text{H}_i$ - ${}^1\text{H}_j$ distance. This dependence is quite sensitive, as it appears as the 6th power of r_{ij} . The rate of spin-lattice relaxation for a single dipole pair obeys simple first-order kinetics and in the case of several interacting protons, the magnetization recovery of proton j after π -pulse inversion (5) is expressible as a sum of exponentials reflecting each single i-j dipole interaction. However, it has been observed (2,6) that for molecules containing many H atoms

$$T_{1j}^{-1} = Af(\omega, \tau_r) \sum_i r_{ij}^{-6} \quad (3)$$

the $\sum_i r_{ij}^{-6}$ term effectively behaves as a geometric parameter (Σ_j) characterizing a magnetization recovery which is well-fitted by a single exponential. Hence, if all the interproton distances are known, eq. (3) indicates that a plot of T_{1j}^{-1} vs. Σ_j should be linear with a slope determined by $Af(\omega, \tau_r)$. Since ω is fixed in a given experiment,

a determination of $Af(\omega, \tau_r)$ affords an estimate of τ_r . Such an analysis of spin-lattice relaxation rates is novel in that usually both τ_r and Σ_j are unknown, severely limiting the applicability of ^1H T_1 determinations when studying biopolymers of uncharacterized or flexible, conformation(s). However, if T_1 data at different fields are available, it is possible to eliminate the distance parameter Σ_j by calculating the ratio $T_1(\omega_1)/T_1(\omega_2) = f(\omega_2, \tau_r)/f(\omega_1, \tau_r)$ containing τ_r as sole unknown (2). Unfortunately, because of instrumental limitations, T_1 field-dependence studies are often not readily accessible, which explains why T_1 determinations on ^{13}C (7,8) or even ^{15}N (9), at fixed field, are usually more informative. The one-bond C-H and N-H distances are assumed known so that, again, only τ_r remains to be determined. For proteins, further ambiguities in the conformational interpretation of the proton relaxation data may arise as a consequence of spin-diffusion (1,3,10,11).

Ferrichrome is a microbial iron-transport ("siderophore") cyclohexapeptide which mediates the metabolic utilization of the metal in a variety of bacteria and fungi (12,13). Alumichrome is an isomorphous (14) analogue of the naturally-occurring coordination compound where Fe^{3+} has been substituted by diamagnetic Al^{3+} . The crystallographic structure of ferrichrome A (15) and ferrichrysin (16), two homologues of ferrichrome which differ in two seryl-for-glycyl substitutions, are known

to 0.2 Å accuracy. For this reason, and because the structure of the coordinated peptides is rigidly maintained in solution (17,18), alumichrome (Fig. 1) has proven to be a unique model system for conformational studies of polypeptide structures by heteronuclear nmr spectroscopy (19-21). From the X-ray coordinates it is possible to position H-atoms on the C-N structural framework by using adequate orbital hybridization to account for the molecular conformation. This enables one to calculate the Σ_j parameters for protons that exhibit well-resolved nmr signals so that the spin-lattice relaxation experiment described above can be performed to independently estimate τ_r from proton T_1 data.

In this communication we report on a series of peptide proton T_1 studies at 100 MHz, 220 MHz and 360 MHz ($B = 2.349$ T, 5.168 T and 8.456 T, respectively). The investigation focused on the amide proton resonances which are usually well resolved and which, because of their chemical shift sensitivity to H-bonding, have become most valuable conformational probes in structural studies by nmr spectroscopy (22-24).

METHODS

The source, preparation and purification of the alumichrome peptides have been reported elsewhere (17-21). In particular, the deferriferrichrome, alumichrome and ^{15}N -alumichrome samples were the same as those used in two previous nmr spin-lattice relaxation studies (8,9). All peptide samples were dissolved to 0.15 M in hexadeutero-dimethylsulfoxide (d_6 -DMSO) after repeated extractions with 8-hydroxyquinoline (8) to remove contaminating paramagnetic metal ions, mainly Fe^{3+} . Consistent with observations of other investigators (25,26), degassing the sample to eliminate O_2 had no detectable effect on the measured proton relaxation rates.

The T_1 's were determined by the $(180-\tau-90-5T_1)_n$ sequence of Vold et al. (5). We have not observed any significant deviation from single exponential behavior in the magnetization recovery after a π -pulse which indicates that eq. (3) is a valid approximation for this study. The measurements at 100 MHz and 360 MHz were performed with a Varian XL-100 and a Bruker HXS-360 spectrometer (ETH-Hönggerberg), respectively. The spectra at 220 MHz were recorded with a Varian HR 220 instrument modified for Fourier performance (UC-Berkeley). Temperatures were determined to $\pm 2^\circ\text{C}$ using a sealed

tube of ethylene glycol standard and the temperature calibration charts provided by the instrument manufacturers. All T_1 's reported here are accurate to better than 5% in the linear least squares standard deviations of the semilogarithmic magnetization recovery plots (correlation coefficients > 0.99).

RESULTS

After π -pulse inversion, the metal-free peptide, deferriferrichrome, exhibits a relatively uniform recovery of the amide ^1H magnetization. Under the specified experimental conditions, Fig. 2 shows that the amide resonances change the magnetization sign at $\tau \sim 160$ ms, the ornithyl doublets appearing to relax somewhat faster ($\langle T_1 \rangle = 238$ ms) than the glycyl triplets ($\langle T_1 \rangle = 300$ ms). Consistent with previous ^{13}C (8,27) and ^{15}N (9) nmr relaxation studies, this indicates that the triglycyl segment is somewhat more flexible than the triornithyl sequence. Furthermore, the similar relaxation rates for each homotripeptide suggest identical dipole-dipole distances for residues within each segment. This would result from a relaxed conformation which accommodates to minimize interatomic repulsive forces thus achieving a distance parameter value which is about equal for all residues of the same kind. The pattern shown by Fig. 2 is reminiscent of the trend

exhibited by the Gramicidin S NH's (23,28), indicative of an overall lack of backbone conformational rigidity for that cyclodecapeptide as well. The situation is drastically different for alumichrome.

After metal complexation the amides become distinct in terms of chemical shifts (14). Concomitantly, Fig. 3 shows that the T_1 values spread over a wider range. As revealed by the $\tau = 160$ ms spectrum, the Orn¹ and Orn² resonances are above the base line when the other four amides are still negative. Thus, while the Gly¹, Gly² and Gly³ NH's relax with $T_1 = 304$ ms, 361 ms and 401 ms, respectively, the ornithyl amides cover a still wider range, with $T_1 = 156$ ms, 221 ms, and 392 ms for Orn², Orn¹ and Orn³, respectively. I.e., once the tertiary structure becomes "frozen" in the metallopeptide, the six amides relax at rates that no longer reflect the particular residue type but rather the distance parameter Σ_j characterizing the dipolar interactions in the rigid spatial structure.

We have studied a variety of deferriferrichrome and alumichrome analogues which differ in the residue occupancy of sites 2 and 3 (alanyl or seryl residues substituting for Gly² and Gly³, Fig. 1) and a consistent pattern has been observed: while the metal-free, flexible cyclohexapeptides show uniform relaxation rates, the Al³⁺-coordinated derivatives exhibit the type of site differentiation exemplified by the spectrum in Fig. 3, and this is independent of temperature (observed at $t = 22^\circ\text{C}$, 45°C , 66°C , 81°C and 97°C). Expectedly, because of a drop in solvent viscosity, all T_1 's become longer at higher temperatures. In what follows, we focus

the discussion on data measured at 44° since earlier ^{13}C and ^{15}N experiments were performed at that temperature (8,9). Table I lists T_1 's at 220 MHz for all the ferrichrome homologues we have studied and shows that the overall amide T_1 pattern remains basically unaffected to the extent that even sites 2 and 3 are essentially insensitive to whether they are occupied by Ala, Gly or Ser residues.

In addition to those at 220 MHz, the amide proton spin-lattice relaxation rates have been measured at 100 MHz and 360 MHz. Fig. 4 shows the $\text{NH } T_{1j}^{-1}$'s at 100 MHz (full circles) plotted against the geometrical dipolar parameter Σ_j calculated from the C,N crystallographic coordinates of ferrichrome A (15) after positioning H atoms using 1.04 Å and 1.09 Å for the N-H and C-H bond distances, respectively (Table II). By least-squares fitting a straight line to the six amide data points, a reasonable match (correlation coeff. = 0.95) between the nmr T_1^{-1} values and the crystallographic Σr^{-6} distance parameter can be obtained:

$$T_{1j}^{-1} = 298.6 \Sigma_j + 1.7 \quad (\text{s}^{-1})$$

The slope measures $A \cdot f(\omega, \tau_r)$ in eq. 3 which, with $\nu = \omega/2\pi = 100$ MHz, directly yields $\tau_r = 4.2 \times 10^{-10}$ s. The intercept at the origin indicate other relaxation processes, extra to ^1H - ^1H dipolar interactions, which are not included in eqs. (1-3).

In a previous communication we have reported on the nitrogen relaxation of ^{15}N -alumichrome at 10.1 MHz and have shown that it is dominantly caused by dipole-dipole interaction with the amide proton. It is hence predictable that the amide ^{14}N - ^1H dipolar interaction

also ought to be sensed by the proton magnetization. We claim that the extra contribution to the amide proton relaxation determined from the ordinate intersect in Fig. 4 is to a great extent due to this heteronuclear dipolar mechanism. This contention is given support by the rate of the Orn³ ¹H^α magnetization recovery. This aliphatic resonance appears well-resolved, next to higher field of the amide region. Fig. 5 shows a partially relaxed spectrum at 360 MHz ($\tau = 240$ ms) spanning the 4.5 ppm $< \delta < 10.5$ ppm spectral region. As illustrated, the amide protons lead the Orn³ ¹H^α in the longitudinal magnetization recovery. In Fig. 4, the Orn³ ¹H^α T_1^{-1} has been included (open circle); as indicated, this aliphatic proton exhibits $\Sigma = 1.33 \times 10^{-2} \text{ \AA}^{-6}$, a distance parameter value which is comparable to those of the Orn³ or Gly³ amide protons (Table II). However, its location on the graph (Fig. 4) is significantly below the position determined by the NH line, the shift being 1.8 s^{-1} , i.e. close to the ordinate intersect value of 1.7 s^{-1} .

Figure 5

The nitrogen dipolar relaxation (4) of the proton magnetization is governed by eq. (4):

$$\left(\frac{1}{T_1}\right)_{\text{NH}} = \frac{4}{30} \hbar^2 \gamma_H^2 \gamma_N^2 \langle r_N^{-6} \rangle I_N (I_N + 1) \left[\frac{\tau_r}{1 + (\omega_H - \omega_N)^2 \tau_r^2} + \frac{3\tau_r}{1 + \omega_H^2 \tau_r^2} + \frac{6\tau_r}{1 + (\omega_H + \omega_N)^2 \tau_r^2} \right] \quad (4)$$

where γ_N is the nitrogen nuclear magnetogyric ratio, I_N the nitrogen nuclear spin, ω_N the nitrogen nmr angular frequency, and r_N is the N-H internuclear distance ($= 1.04 \text{ \AA}$). Assuming that the ¹⁴N-¹H dipolar interaction is the only relaxation mechanism besides ¹H-¹H dipolar interactions, the intersect value in Fig. 4 yields, on the basis of eq. (4), an independent estimate

of the isotropic rotational correlation time, $\tau_r = 2.8 \times 10^{-10}$ s, which is close to that derived from the linear fit slope, $\tau_r = 4.2 \times 10^{-10}$ s.

Independent evidence for the role of nitrogen in determining the amide relaxation, is afforded by comparing ^1H longitudinal relaxation rates determined from ^{14}N (natural abundance) and 99.2% ^{15}N -enriched peptides. Inserting the proper parameter values characterizing the two nitrogen isotopes [$I = 1$ (^{14}N), $1/2$ (^{15}N); $\gamma = 0.1934$ (^{14}N), -0.2712 (^{15}N) rad/sT; $\nu = 15.89$ (^{14}N), 22.29 (^{15}N) MHz for 220 MHz (^1H)] into eq. (4), one can predict that the nitrogen dipolar contribution to the proton T_1^{-1} should decrease by a factor of ca. 0.73 on going from the ^{14}N to the ^{15}N peptide. In other words, the ^{14}N and ^{15}N peptides ought to yield similar dependencies when plotting T_{1j}^{-1} vs. Σ_j but with the ^{15}N peptide line displaced below that of the ^{14}N peptide. Comparing the relaxation rates of alumichrome and ^{15}N -alumichrome (Table I) the predicted trend is seen to be satisfied by each of the amides.

Figure 6 shows the T_1^{-1} vs Σ plot for both peptides at 220 MHz, the linear least squares fits yielding

$$T_1^{-1} = 143.7 \Sigma + 1.6 \text{ s}^{-1} \quad (^{14}\text{N-peptide})$$

and

$$T_1^{-1} = 112.8 \Sigma + 1.3 \text{ s}^{-1} \quad (^{15}\text{N-peptide})$$

both with correlation coefficients = 0.95. [Ideally, both lines should be parallel. The discrepancy most likely reflects experimental errors and the effect of fitting the magnetization recoveries with single exponentials.]

The field dependence of the amide proton spin-lattice relaxation shows that T_1 's become longer at higher frequencies (Table II) while the

Figure 7 slopes of the linear fits decrease (Fig. 7). This is what would be expected from the ω -dependence of $f(\omega, \tau_r)$, and it indicates the fact that at high fields cross relaxation (10,11) becomes important, the Σ parameter playing a lesser role in determining the relaxation individuality of each amide.

DISCUSSION

As presented above, each linear fit provides two independent estimates of τ_r , one from the slope value (^1H - ^1H interaction) and the other from the intersect (^1H - ^{14}N or ^1H - ^{15}N interaction). From the data on ^{14}N - and ^{15}N -alumichrome at 100, 220, and 360 MHz (Figs. 6 and 7) four linear fits were obtained and eight independent τ_r estimates derived (Table III), with an average $\langle \tau_r \rangle = 3.58 \times 10^{-10}$ s. Confirming this estimate, $\langle \tau_r \rangle = 3.97 \times 10^{-10}$ s was independently derived from the ratios of slopes and intersects at any two fields. The overall internal consistency of these independent estimates is gratifying, especially if one considers that T_1 determinations on other heteronuclei have yielded $\langle \tau_r \rangle \sim 4.1 \times 10^{-10}$ s (^{13}C) and $\langle \tau_r \rangle \sim 3.8 \times 10^{-10}$ s (^{15}N) for alumichrome under identical solution conditions (8,9).

Table III

The two ferrichrome crystallographic studies reported to date (15,16) conclude essentially identical molecular shapes except, mainly, in the configuration of the Orn¹ amide. In the case of ferrichrome A (15) this NH is pointing towards the pouch defined by the cyclohexapeptide backbone ring and the three ornithyl sidechains. The amide hydrogen atom is hence surrounded by a lipophilic enclosure and is considerably isolated from direct interaction with the molecular exterior. The picture is essentially repeated in crystalline ferrichrysin (16), only that by rotating to a 19° larger ϕ angle, the Orn¹ NH points closer to the Orn³ δ -N-hydroxy oxygen atom (N...O distance $\sim 3.2 \text{ \AA}$) suggesting the possibility of another H-bond. The authors (16) have speculated that this other H-bond would confer extra conformational stability to the molecule. Ferrichrome A and ferrichrysin both possess the same amino acid composition, the only difference being the hydroxamate acyl substituent which is trans- β -methyl glutaconic acid in the first and acetic acid in the second (12). Except for resonances arising from the hydroxamate groups, the proton nmr spectra of alumichrome A and alumichrysin are essentially superimposable. The spectra do not reveal any difference in the extent of H bonding at the Orn¹ NH (18,29). NMR investigations of a variety of alumichrome homologues, which differ in the residue occupancy of sites 2 and 3 (Fig. 1) and/or in the nature of the coordinated ion (Al³⁺, Ga³⁺, or Co³⁺, (17,18,24)) always detect the Orn¹-NH-proton-resonance at significantly higher fields, ca. 3.4 ppm closer to the TMS reference signal, than the strongly intramolecularly H-bonded Orn² NH resonance (Fig. 3). Furthermore, a variety of heteronuclear solvent perturbation

experiments (19,21,24) and the positive slope of the temperature dependence of the amide proton resonance chemical shift, provide support to a model where the $\text{Orn}^1 \text{NH}$ does not interact with the solvent and it is not intramolecularly H bonded. When plotting the proton T_1^{-1} vs. the distance parameter Σ calculated from the ferrichrysin crystallographic coordinates (16) we consistently find larger deviations (correlation coeff. ~ 0.7) for the linear least squares fit than when using the ferrichrome A coordinates (correlation coeff. > 0.9). The discrepancy arises mainly from the exceedingly high values attributed to the $\text{Orn}^1 \text{NH}$ Σ by the ferrichrysin coordinates because of positioning this proton closer to the ornithyl sidechain methylene protons ($\Sigma \approx 0.0452 \text{ \AA}^{-1}$). It

thus appears that for solution conditions, the crystallographic model of Zalkin et al. (15) better reflects the fine details of the molecular conformation of all the Al^{3+} , Ga^{3+} and Co^{3+} ferrichrome analogues examined to date. Given the similarity of the Ga^{3+} , Co^{3+} and Fe^{3+} ionic radius ($r_0 = 0.63 \text{ \AA}$ (30)) it is likely that the $\text{Orn}^1 \text{NH}$ be not H bonded in the ferric complex either and that the hindrance of this amide to H-exchange with the solvent (14) is a consequence of its buried location only. The 6th power distance sensitivity of the nmr spin-lattice relaxation rate strongly supports this view and should, in other structurally rigid peptides, afford a definite test of proposed conformational models.

The influence of $^1\text{H}-^{14}\text{N}$ dipolar interactions on the overall amide proton relaxation rates can have important consequences for the analysis of intramolecular $^1\text{H}-\{^1\text{H}\}$ nuclear Overhauser effect data. Norton and Allerhand (31) have shown that in the case

of non-protonated carbon atoms, the ^{13}C - ^{14}N dipolar interaction can govern the ^{13}C T_1 and hence significantly affect the magnitude of ^{13}C - $\{^1\text{H}\}$ nOe's. As we are showing, ^{14}N dipolar interaction also affects the amide ^1H T_1 so that the effective ^1H - $\{^1\text{H}\}$ nOe between, e.g. NH and C^αH , will be similarly reduced. Fig. 4 shows that even though the ^{14}N - ^1H relaxation is the same for all the amide protons, it represents a variable fraction of the measured overall proton relaxation rates. As exemplified by the Orn³ amide, it can even be a major contributor to the observed NH proton relaxation rate. On the basis of the study of Bell and Saunders (33), ^1H - $\{^1\text{H}\}$ nOe's are being increasingly exploited to derive dihedral angle and distance information in conformational investigations of peptide structures (34 and references therein). The present study calls for caution in interpreting such data when amide NH protons are observed in the nOe experiment. Since the relative contribution of the ^{14}N dipolar mechanism increases with frequency, at high fields the net amide ^1H - $\{^1\text{H}\}$ nOe loses significance as a direct measure of molecular geometry. Yet, even under such unfavorable conditions, the r^{-6} dependence does manifest itself as a rate-determining factor in the buildup of the ^1H - $\{^1\text{H}\}$ nOe (35), however small the latter may be. This points towards a need to re-evaluate interpretations of reported NH nOe's and to plan future such experiments accordingly.

Acknowledgements The authors are indebted to Mr. W. Meier for his collaboration in preliminary aspects of this project and to Dr. E. S. de Llinás for computational assistance. Mr. R. Baumann, Dr. W. J. Horsley and Dr. A. de Marco provided valuable help with the nmr spectroscopic work. This project was sponsored by the Division of Biological and Environmental Research of the U.S. Department of Energy, the N.I.H. (Grant NCI-1-RO-1-CA1428-1), and the Swiss N.S.F. (Grant 3.131.73).

REFERENCES

1. Kimmich, R., and F. Noak. 1971. Nuclear magnetic relaxation in solutions of proteins and polypeptides. Ber. Bunsengesellschaft Phys. Chem. 75:269-272.
2. Coates, H. B., K. A. McLauchlan, I. D. Campbell, and C. E. McColl. 1973. Proton spin lattice relaxation time measurements at 90 MHz and 270 MHz. Biochim. Biophys. Acta 310:1-10.
3. Sykes, B. D., W. E. Hull, and G. H. Snyder. 1978. Experimental evidence for the role of cross-relaxation in proton nuclear magnetic resonance spin lattice relaxation time measurements in proteins. Biophys. J. 21:137-146.
4. Solomon, I. 1955. Relaxation processes in a system of two spins. Phys. Rev. 99:559-565
5. Vold, R. L., J. S. Waugh, M. P. Klein and D. E. Phelps. 1968. Measurement of spin relaxation in complex systems. J. Chem. Phys. 48:3831-3832.
6. Gutowsky, H. S., and D. E. Woessner. 1956. Nuclear magnetic spin-lattice relaxation in liquids. Phys. Rev. 104:843-844.
7. Lyster, J. R., and G. C. Levy. 1974. Carbon-13 nuclear spin relaxation. Topics in Carbon-13 NMR Spectroscopy 1:79-148.
8. Llinás, M., W. Meier, and K. Wüthrich. 1977. A carbon-13 spin lattice relaxation study of alumichrome at 25.1 MHz and 90.5 MHz. Biochim. Biophys. Acta 492:1-11.
9. Llinás, M., and K. Wüthrich. 1978. A nitrogen-15 spin-lattice relaxation study of alumichrome. Biochim. Biophys. Acta 532:29-40.

10. Kalk, A., and H. J. C. Berendsen. 1976. Proton magnetic relaxation and spin diffusion in proteins. J. Magn. Resonance 24:343-366.
11. Bothner-By, A. A., and P. M. Johner. 1977. Spin-diffusion in macromolecules and its effect on nuclear Overhauser effects in proteins. Proceedings XX C.S.I. and 7 I.C.A.S., Prague, pp 355-372.
12. Neilands, J. B. 1973. Microbial Iron Transport Compounds, Chapter V in "Inorganic Biochemistry", G. L. Eichhorn Ed., Elsevier, Amsterdam.
13. Emery, T. 1974. Biosynthesis and Mechanism of Action of Hydroxamate-type Siderochromes, Chapter 5 in "Microbial Iron Metabolism", J. B. Neilands Ed., Academic, New York.
14. Llinás, M. 1973. Metal-polypeptide interactions: the conformational state of iron proteins. Struct. Bonding 17:139-151.
15. Zalkin, A., J. D. Forrester, and D. H. Templeton. 1966. Ferrichrome-A tetrahydrate. Determination of crystal and molecular structure. J. Amer. Chem. Soc. 88:1810-1817.
16. Norrestam, R., B. Stensland, and C. I. Brändén. 1975. On the conformation of cyclic iron-containing hexapeptides: The crystal and molecular structure of ferrichrysin. J. Molec. Biol. 99:501-506.
17. DeMarco, A., M. Llinás, and K. Wüthrich. 1978. Analysis of the ^1H -NMR spectra of ferrichrome peptides (I): the non-amide protons. Biopolymers 17:617-636.
18. DeMarco, A., M. Llinás, and K. Wüthrich. 1978. Analysis of the ^1H -NMR spectra of ferrichrome peptides (II): the amide resonances, Biopolymers 17:637-650.

19. Llinás, M., W. J. Horsley, and M. P. Klein. 1976. Nitrogen-15 nuclear magnetic resonance spectrum of alumichrome detection by a double resonance Fourier transform technique. J. Amer. Chem. Soc. 98: 7554-7558.
20. Llinás, M., D. M. Wilson, and J. B. Neilands. 1977. Peptide strain. Conformation dependence of the carbon-13 nuclear magnetic resonance chemical shifts in the ferrichromes. J. Amer. Chem. Soc. 99:3631-3637.
21. Llinás, M., D. M. Wilson, and M. P. Klein. 1977. Peptide hydrogen bonding. Conformation dependence of the carbonyl carbon-13 nuclear magnetic resonance chemical shifts in ferrichrome. A study by $^{13}\text{C}\{-^{15}\text{N}\}$ Fourier double resonance spectroscopy. J. Amer. Chem. Soc. 99:6846-6850.
22. Urry, D. W., and M. Ohnishi. 1970. Nuclear magnetic resonance and the conformation of cyclic polypeptide antibiotics. in "Spectroscopic Approaches to Biomolecular Conformations", D. W. Urry, Ed., p 263-300 Chicago: A.M.A.
23. Wyssbrod, H. R., and W. A. Gibbons. 1973. Conformation-function relationship in peptides and proteins. Survey Progr. Chem. 6:209-325.
24. Llinás, M., and M. P. Klein. 1975. Charge relay at the peptide bond. A proton magnetic resonance study of solvation effects on the amide electron density distribution. J. Amer. Chem. Soc. 97:4731-4737.
25. Cutnell, J. D., J. A. Glasel, and V. J. Hruby. 1975. An investigation of contributions to carbon-13 spin-lattice relaxation in amino acids and peptide hormones". Org. Mag. Resonance 7:256-261.

26. Pitner, T. P., J. D. Glickson, R. Rowan, J. Dadok, and A. A. Bothner-By. 1975. Delineation of interactions between specific solvent and solute nuclei. A nuclear magnetic resonance solvent saturation study of Gramicidin S in methanol, dimethyl sulfoxide, and trifluoroethanol. J. Amer. Chem. Soc. 97:5917-5918.
27. Deslauriers, R., G. C. Levy, W. H. McGregor, D. Sarantakis, and I. C. P. Smith. 1977. The influence of glycyI residues on the flexibility of peptide hormones in solution. Eur. J. Biochem. 75:343-346.
28. Redfield, A. G., and R. K. Gupta. 1971. Pulsed-Fourier-transform nuclear magnetic resonance spectrometer. Adv. Magnetic Resonance 5:82-115.
29. Llinás, M., M. P. Klein, and J. B. Neilands. 1972. Solution conformation of the ferrichromes III. A comparative proton magnetic resonance study of glycine- and serine-containing ferrichromes. J. Mol. Biol. 68:265-284.
30. Crystal ionic radii of the elements, in Handbook of Chemistry and Physics, 52nd. Edition, R. C. Weast, Ed., 1971, p F-171, The Chemical Rubber Co., Ohio.
31. Norton, R. S., and A. Allerhand. 1976. Effect of ^{13}C - ^{14}N dipolar interactions on spin-lattice relaxation times and intensities of nonprotonated carbon atoms. J. Amer. Chem. Soc. 98:1007-1014.
32. Noggle, J. H., and R. E. Schirmer. 1971. The nuclear Overhauser effect. Academic Press, New York.
33. Bell, R. A., and J. K. Saunders. 1970. Correlation of the intramolecular nuclear Overhauser effect with internuclear distance. Can. J. Chem. 48:1114-1122.

34. Bothner-By, A. A. (in press). Nuclear Overhauser effects in protons, and their use in the investigation of structures of biomolecules. in "Magnetic Resonance Studies in Biology", R. G. Shulman, Ed. Academic, New York.
35. Freeman, R., H. D. W. Hill, and R. Kaptein. 1972. Proton-decoupled nmr spectra of carbon-13 with the nuclear Overhauser effect suppressed. J. Mag. Res. 7:327-329.

Table I

AMIDE PROTON SPIN-LATTICE RELAXATION TIMES OF ALUMICHROME HOMOLOGUES

	Gly ¹	Site 2	Site 3	Orn ¹	Orn ²	Orn ³
Alumichrome	223	264 (G)	275 (G)	166	134	278
Alumichrome C	203	269 (A)	258 (G)	164	132	286
Alumicrocin	199	245 (S)	282 (G)	179	135	259
Alumisake	236	258 (A)	244 (S)	171	123	279
Alumichrysin	210	239 (S)	230 (S)	162	145	281
Alumichrome- ¹⁵ N	271	293 (G)	334 (G)	253	162	369

T_1 values (ms) determined at 220 MHz, 0.15 M solutions in d_6 -DMSO at 44°C.

Residue occupancy of sites 2 and 3 are indicated in parenthesis: A, alanine; G, glycine; S, serine.

Table II

ALUMICHROME AMIDE DISTANCE PARAMETERS AND FIELD DEPENDENCE
OF THE RELAXATION RATES

	$\Sigma r_{\text{HH}}^{-6}$ ($\text{\AA}^{-6} \times 10^2$)	T_1^{-1} (s^{-1})		
		100 MHz	220 MHz	360 MHz
Gly ¹	1.93	7.02	4.48	2.94
Gly ²	1.49	6.62	3.78	2.58
Gly ³	2.03	5.93	3.64	2.42
Orn ¹	2.62	10.47	6.02	3.60
Orn ²	4.14	13.70	7.46	4.46
Orn ³	1.25	5.66	3.60	2.33

Table III

LEAST SQUARES FIT $T_1^{-1} = A + f(\omega, \tau_r) \Sigma r_{HH}^{-6}$:

PARAMETERS AND DERIVED τ_r VALUES

Peptide	$\omega/2\pi$	intersect data		slope data	
		A	τ_r	$f(\omega, \tau_r)$	τ_r
¹⁴ N-Alumichrome	100 MHz	1.69	2.79	291.59	4.20 ^a
	220 MHz	1.61	3.07	143.69	2.19 ^b
	360 MHz	1.35	4.28	75.83	7.23
¹⁵ N-Alumichrome	220 MHz	1.29	3.51	112.84	1.35 ^b

Units: A, s⁻¹; $f(\omega, \tau_r)$, Å⁶ s⁻¹; τ_r , s x 10¹⁰. The correlation coefficients for the least squares fits were in all cases > 0.95

(a) Highest of two possible values. (b) Lowest of two possible values.

FIGURE CAPTIONS

Figure 1. Structure of the ferrichromes.¹⁴⁻¹⁶ The model represents ferrichrome C. Peptide backbone bonds are denoted in heavier trace and H bonds by dotted lines (.....). For the present study Fe^{3+} was substituted by Al^{3+} . The alumichrome homologues investigated differ in the residue occupancy of sites 2 and 3 as follows:

	site 2	site 3
Alumichrome	Gly	Gly
Alumichrome C	Ala	Gly
Alumicrocin	Ser	Gly
Alumisake	Ala	Ser
Alumichrysin	Ser	Ser

Figure 2. Sequence of partially relaxed spectra of deferriferrichrome at 220 MHz (0.15 M in d_6 -DMSO, $t \approx 81^\circ\text{C}$). The six amide signals appear between ca 7.5 ppm and 8.3 ppm. Gly NH resonances triplets appear at lower field from the ornithyl doublet positions. The broad resonance at ~ 9.3 ppm arises from the free hydroxamic acid NOH group. Measured T_1 values are indicated. The spectrum has been described elsewhere [(14) and ref. therein].

Figure 3. Sequence of partially relaxed spectra of alumichrome at 220 MHz (0.15 M in d_6 -DMSO, $t \approx 81^\circ\text{C}$). Resonance assignments and measured T_1 values are indicated. The spectrum has been described elsewhere (14,18).

Figure 4. Linear least squares plot of T_1^{-1} versus distance parameter Σ from the alumichrome amides (100 MHz, 0.15 M solution in d_6 -DMSO, $t = 44^\circ\text{C}$). NH data are represented by full circles (\bullet) while the $^3\text{C}_\alpha$ measurement, not considered in the linear fit, is denoted by an open circle (\circ). Experimental uncertainties are included. The data are listed in Tables II and III.

Figure 5. Partially relaxed spectrum of the low field resonance region of alumichrome at 360 MHz ($\tau = 240$ ms, 0.15 M in d_6 -DMSO, $t = 44^\circ\text{C}$).

Figure 6. Linear least squares plot of T_1^{-1} versus distance parameter Σ for ^{14}N - and ^{15}N -alumichrome (220 MHz, 0.15 M solutions in d_6 -DMSO, $t = 44^\circ\text{C}$). The data are listed in Tables I and III.

Figure 7. Field dependence of the alumichrome amide NH^1H -NMR spin-lattice relaxation. Linear least squares plots of T_1^{-1} versus distance parameter Σ (0.15 M solution, $t = 44^\circ\text{C}$). The data are listed in Tables II and III.

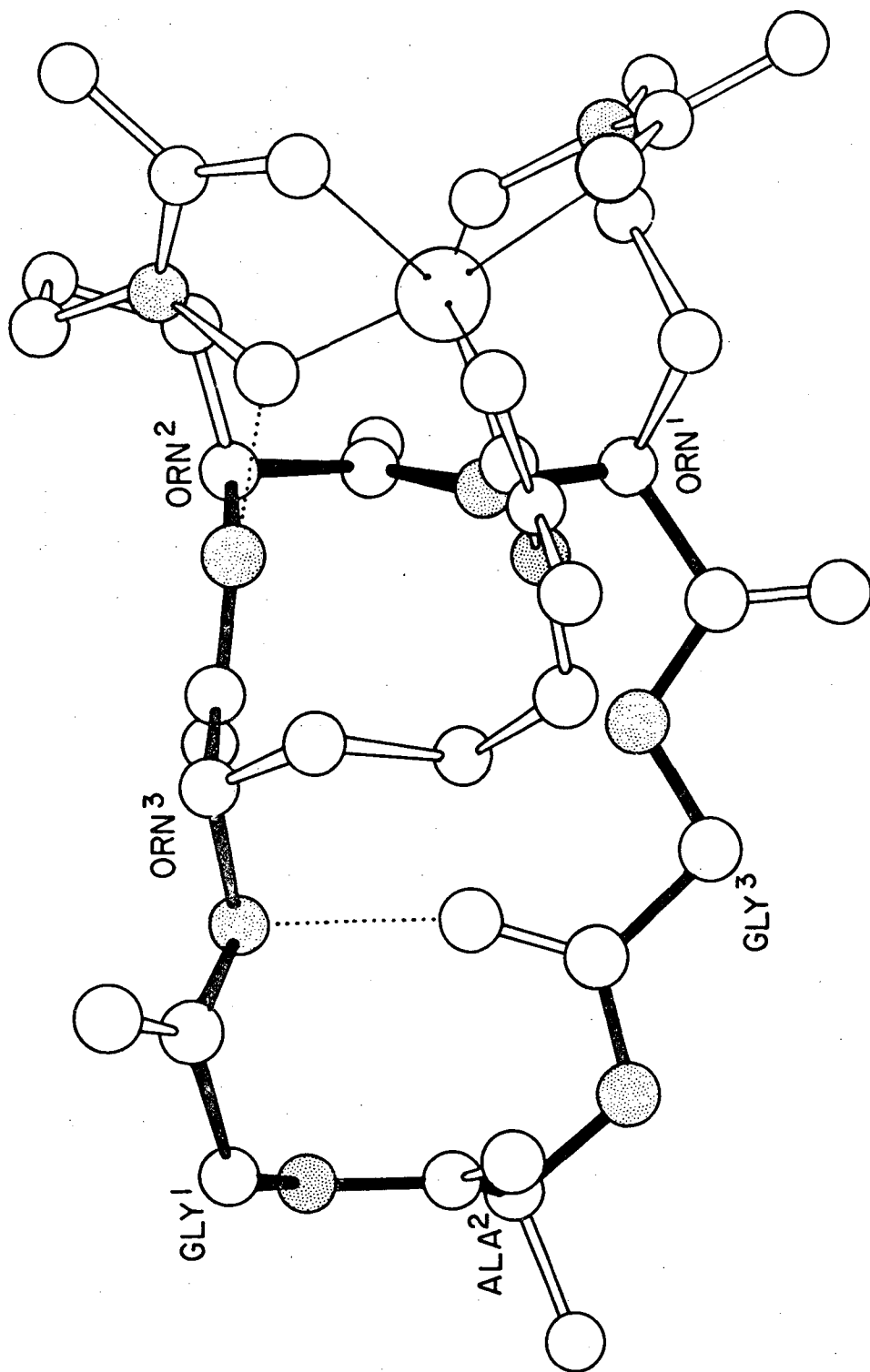
FERRICHROME C

Fig. 1

	T_1 (sec)	T_1 (sec)
Gly ₁	0.309	Orn ₁ 0.246
Gly ₂	0.292	Orn ₂ 0.225
Gly ₃	0.299	Orn ₃ 0.243

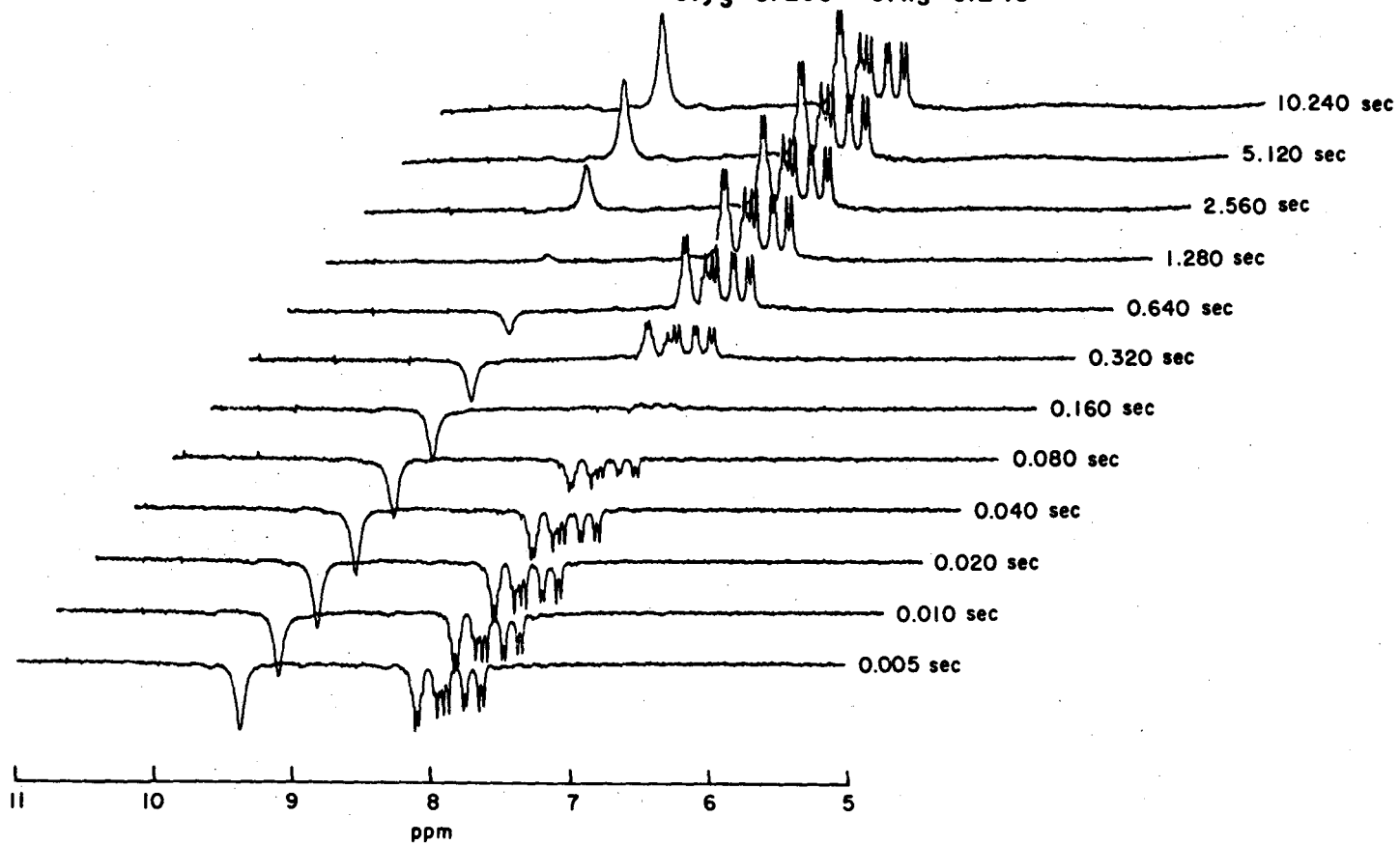


Fig. 2

Orn ₂	Gyl ₁	Gyl ₂	Orn ₃	Gyl ₃	Orn ₁
T ₁ (sec)=0.156	0.304	0.361	0.392	0.401	0.221

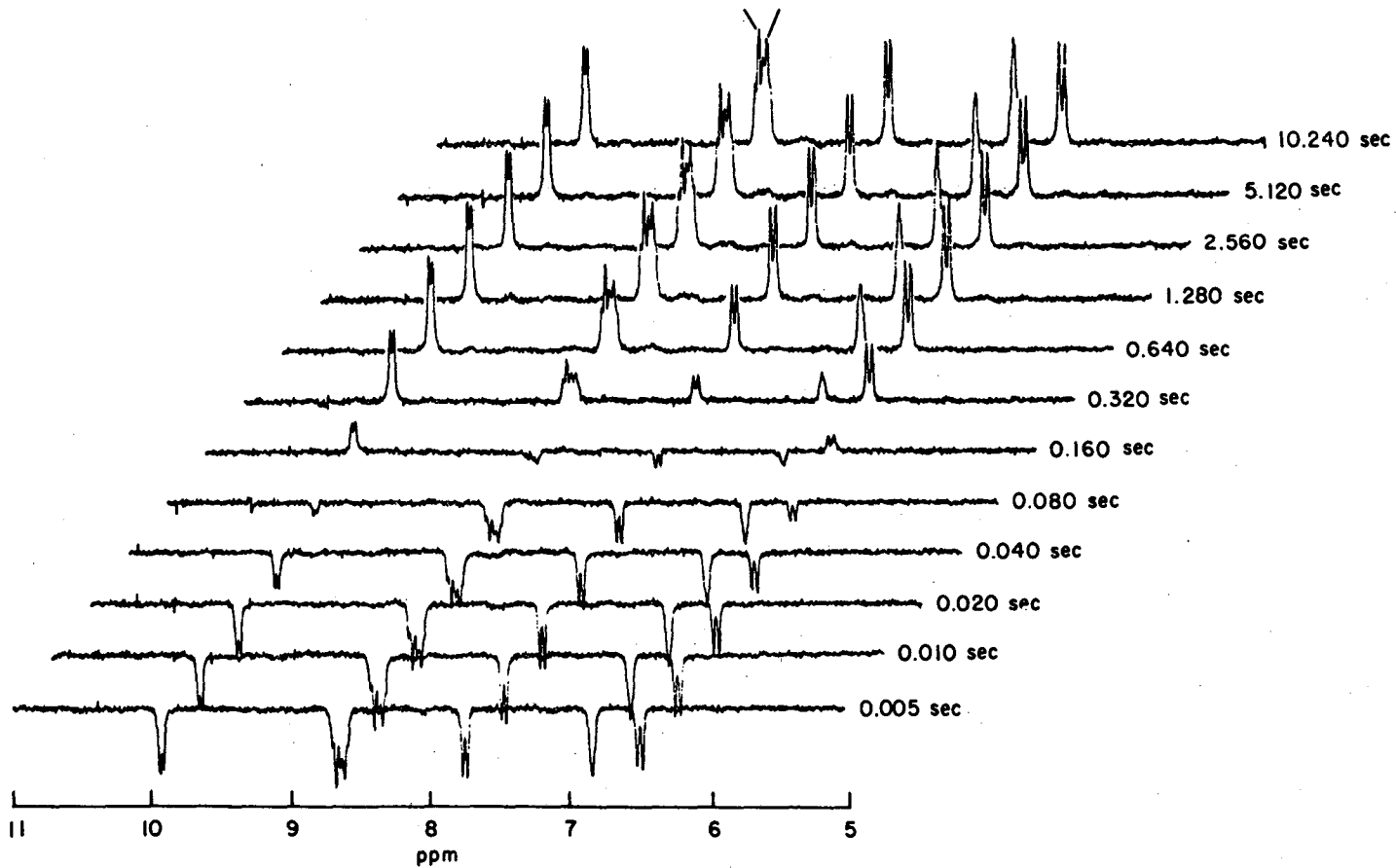


Fig. 3

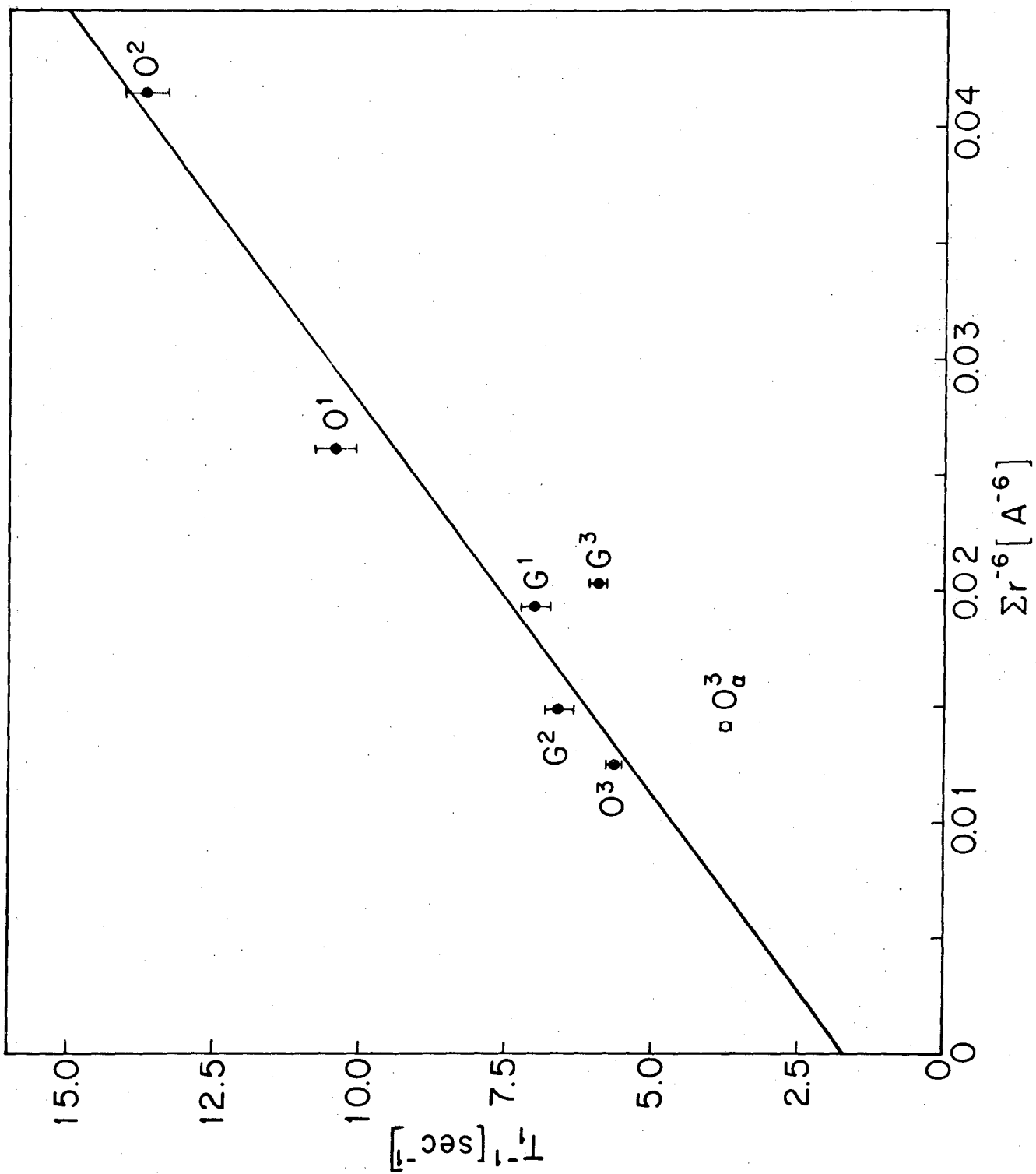


Fig. 4

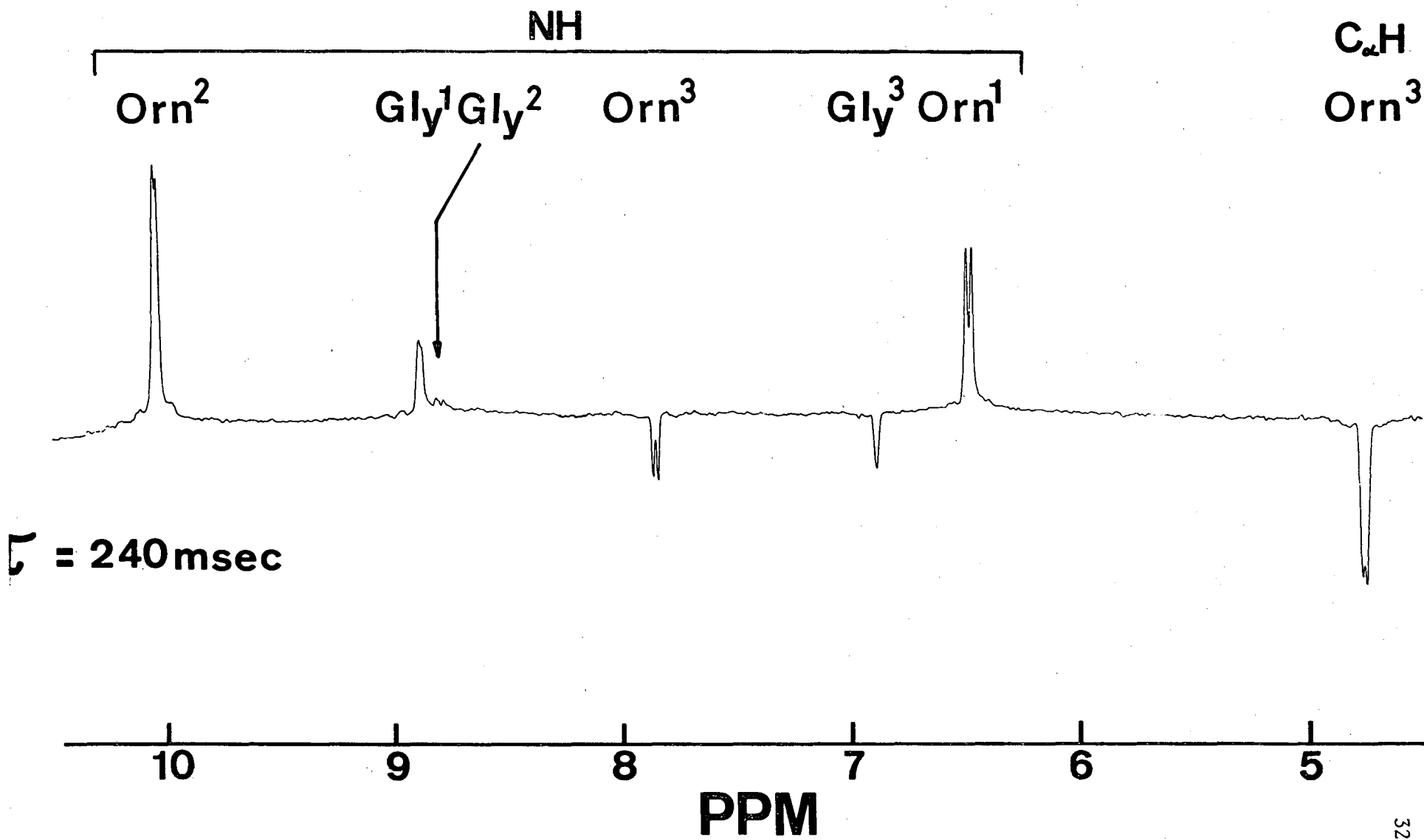


Fig. 5

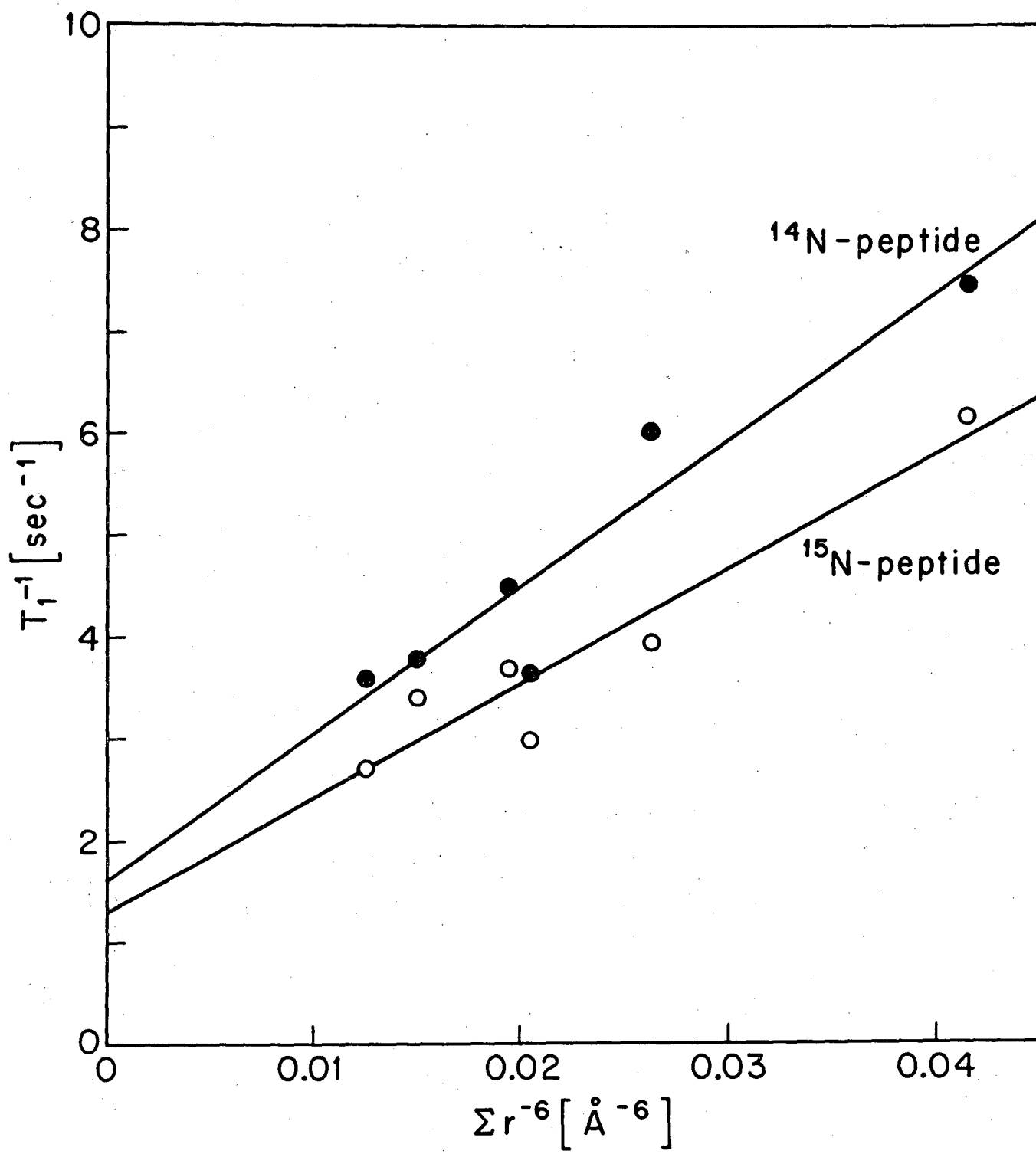


Fig. 6

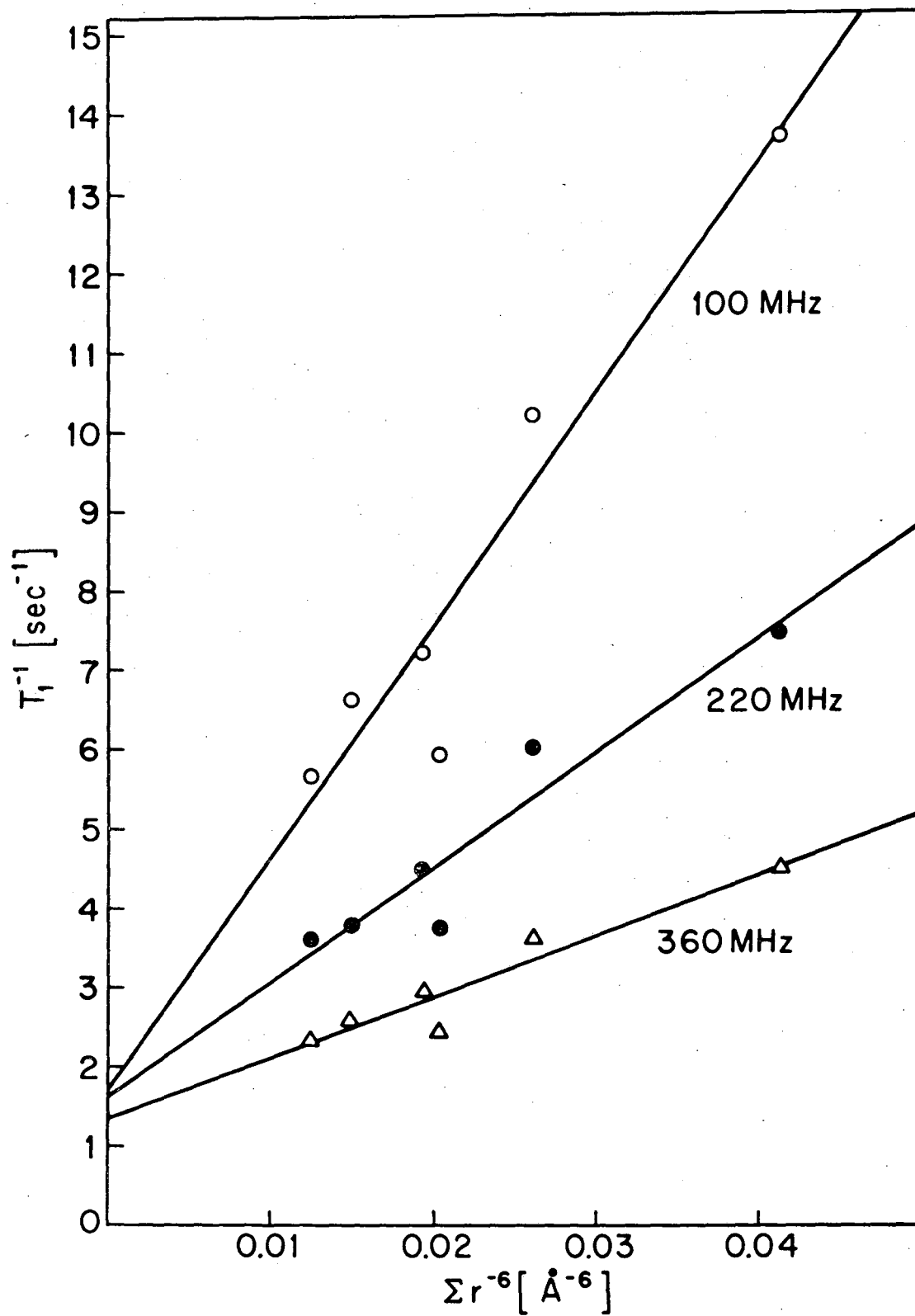


Fig. 7

This report was done with support from the Department of Energy. Any conclusions or opinions expressed in this report represent solely those of the author(s) and not necessarily those of The Regents of the University of California, the Lawrence Berkeley Laboratory or the Department of Energy.

TECHNICAL INFORMATION DEPARTMENT
LAWRENCE BERKELEY LABORATORY
UNIVERSITY OF CALIFORNIA
BERKELEY, CALIFORNIA 94720